


Knockdown of Annexin A1 Enhances Radioresistance and Inhibits Apoptosis in Nasopharyngeal Carcinoma

Technology in Cancer Research & Treatment
Volume 17: 1–10
© The Author(s) 2018
Reprints and permission:
sagepub.com/journalsPermissions.nav
DOI: 10.1177/1533034617750309
journals.sagepub.com/home/tct


Li Liao, PhD^{1,2}, Wen-Jing Yan, MS², Chun-Mei Tian, MS²,
Mao-Yu Li, PhD³, Yong-Quan Tian, PhD¹, and Gu-Qing Zeng, PhD²

Abstract

Radiotherapy is the primary treatment for nasopharyngeal carcinoma while radioresistance can hinder efficient treatment. To explore the role of annexin A1 and its potential mechanisms in radioresistance of nasopharyngeal carcinoma, human nasopharyngeal carcinoma cell line CNE2-sh annexin A1 (knockdown of annexin A1) and the control cell line CNE2-pLKO.1 were constituted and CNE2-sh annexin A1 xenograft mouse model was generated. The effect of annexin A1 knockdown on the growth of xenograft tumor after irradiation and radiation-induced DNA damage and repair was analyzed. The results of immunohistochemistry assays and Western blotting showed that the level of annexin A1 was significantly downregulated in the radioresistant nasopharyngeal carcinoma tissues or cell line compared to the radiosensitive nasopharyngeal carcinoma tissues or cell line. Knockdown of annexin A1 significantly promoted CNE2-sh annexin A1 xenograft tumor growth compared to the control groups after irradiation. Moreover, the terminal deoxynucleotidyl transferase-mediated dUTP nick end labeling assays revealed that knockdown of annexin A1 significantly inhibited apoptosis *in vivo* compared to the control groups. We assessed the intracellular reactive oxygen species levels and the extent of radiation-induced DNA damage and repair using reactive oxygen species assay, comet assays, and immunohistochemistry assay. The results showed that knockdown of annexin A1 remarkably reduced the intracellular reactive oxygen species levels, level of DNA double-strand breaks, and the phosphorylation level of H2AX and increased the accumulation of DNA-dependent protein kinase in nasopharyngeal carcinoma cells after irradiation. The findings suggest that knockdown of annexin A1 inhibits DNA damage via decreasing the generation of intracellular reactive oxygen species and the formation of γ -H2AX and promotes DNA repair via increasing DNA-dependent protein kinase activity and therefore improves the radioresistance in nasopharyngeal carcinoma cells. Together, our findings suggest that knockdown of annexin A1 promotes radioresistance in nasopharyngeal carcinoma and provides insights into therapeutic targets for nasopharyngeal carcinoma radiotherapy.

Keywords

annexin A1, apoptosis, radioresistance, DSBs, DNA-PKcs, nasopharyngeal carcinoma

Abbreviations

ANXA1, annexin A1; CR, complete remission; DCF-DA, 2',7'-dichlorofluorescein diacetate; DMEM, Dulbecco's modified Eagle medium; DNA-PKcs, DNA-dependent protein kinase; DSBs, double-strand breaks; HNSCC, head and neck squamous cell carcinoma; IR, ionizing radiation; NPC, nasopharyngeal carcinoma; PD, progression disease; PR, partial remission; ROS, reactive

¹ School of Public Health, Central South University, Changsha, Hunan, China

² School of Nursing, University of South China, Hengyang, Hunan, China

³ Key Laboratory of Cancer Proteomics of Chinese Ministry of Health, Xiangya Hospital, Central South University, Changsha, Hunan, China

Corresponding Authors:

Gu-Qing Zeng, PhD, School of Nursing, University of South China, 28# Changsheng Road West, Hengyang, Hunan 421001, China.

Email: zengguqing0123@163.com

Yong-Quan Tian, PhD, School of Public Health, Central South University, Changsha, Hunan 410078, China.

Email: tianyq@csu.edu.cn



oxygen species; SD, stable disease; shRNA, short hairpin RNA; TUNEL, terminal deoxynucleotidyl transferase (TdT)-mediated dUTP nick end labeling.

Received: July 26, 2017; Revised: November 15, 2017; Accepted: November 22, 2017.

Introduction

Nasopharyngeal carcinoma (NPC) is the most common cancer originating in the nasopharynx, which is highly prevalent in southern China and Southeast Asia. Despite recent advances in radiotherapy, one of the primary treatments for NPC,¹ it has been widely used in the treatment of patients with NPC, yet outcomes still remain poor in certain cases. Radioresistance is believed to be the main potential reason to hinder the efficiency of radiotherapy.² The mechanism underlying the radioresistance of NPC remains largely unknown. Therefore, to identify predictive markers of radioresistance and explore efficient targets for radiosensitization may contribute to improving radiotherapy effect on patients with NPC.

Annexin A1 (ANXA1), a Ca²⁺-regulated phospholipid-binding protein of the annexin superfamily, is involved in the regulation of numerous cell processes, such as cell proliferation, apoptosis, and metastasis.³ The dysregulation of ANXA1 was widely reported in a large number of malignant tumors, such as breast cancer, pancreatic cancer, and non-small cell lung cancer.^{4,5} In head and neck squamous cell carcinoma (HNSCC), ANXA1 may act as a tumor suppressor, and its expression is correlated with less aggressive tumors or higher grades of differentiation.⁶ Although upregulation of endogenous ANXA1 promotes cell death,⁷ its role for the progression and radioresistance in NPC is poorly clear.

In this study, immunohistochemistry assays and Western blotting were performed to assess the expression of ANXA1 in radioresistant and radiosensitive NPC tissues or cell lines. The effects of knockdown of ANXA1 on radioresistance in NPC *in vivo* were investigated by using a xenograft model via injecting the CNE2-shANXA1 cells or the control cells subcutaneously into the flank of nude mice, respectively. Additionally, the key molecular markers were detected to be involved in double-strand breaks (DSBs) to approach the potential mechanism of ANXA1 in radioresistance of NPC. In conclusion, our data suggest that ANXA1 is relevant to radioresistance of NPC and may provide potential therapeutic targets for NPC radiotherapy.

Materials and Methods

Tissues

A total of 86 cases of NPC tissues (41 radioresistant NPC tissues, 45 radiosensitive NPC tissues) were obtained from the First and Second Affiliated Hospital of University of South China, China. The patients were clinically diagnosed by experts from the department of otolaryngology and

pathologically diagnosed by experts from the department of pathology. All tissues were examined for immunohistochemistry. All patients were examined for cancer regression in the neck and nasopharynx (nasal endoscopy and nasopharyngeal computed tomography examination), 3 months after the completion of radiotherapy. The short-term therapeutic evaluation of radiotherapy was evaluated according to the international standard as follows: complete remission (CR): tumor disappeared, the nasopharynx soft tissue returned to normal; partial remission (PR): the tumor disappeared over 50%, most of the nasopharyngeal structures returned to normal; stable disease (SD): tumor volume decreased <50%, most of the nasopharyngeal structures did not return to normal; progression disease (PD): tumor volume increased. The criteria for defining the clinically radioresistant and radiosensitive patients were as follows: the patients with CR and PR were considered the clinically radiosensitive patients and the patients with SD and PD were thought to be the clinically radioresistant patients.⁸ The clinicopathologic features of the patients used in the present study are shown in Table 1. The study was approved by the local ethical committee and the informed consent forms were obtained from patients.

Cell Lines and Cell Culture

Human NPC cell line CNE2-IR (radioresistant subclone cell line) and control cell line CNE2 were established by us⁹ and used in this study. Cells were normally maintained in Dulbecco's modified Eagle medium (DMEM) medium (Invitrogen, Carlsbad, California) supplemented with 10% fetal bovine serum (Invitrogen).

Immunohistochemistry and Evaluation of Staining

Immunohistochemistry was done on formalin-fixed and paraffin-embedded tissue specimens including 41 radioresistant NPC tissues and 45 radiosensitive NPC tissues (radioresistance of NPC tissues and radiosensitivity of NPC tissues were obtained from hospital medical records). Briefly, 4 μ m of tissue sections were deparaffinized, rehydrated, and treated with an antigen retrieval solution (10 mmol/L sodium citrate buffer, pH 6.0). The sections were incubated with anti-ANXA1 (1:500; Sigma-Aldrich, St Louis, Missouri) antibody overnight at 4°C and then were incubated with 1:1000 dilution of biotinylated secondary antibody. Immunoreactivity was visualized using 3',3'-diaminobenzidine tetrachloride (Sigma-Aldrich) and counterstained with hematoxylin. In negative controls, primary antibodies were replaced by phosphate buffer saline.

Table 1. The Clinical and Pathological Characteristics of the Radio-resistant and Radiosensitive Patients With NPC.

	Radiosensitive NPC Tissues (n = 45)	Radioreistant NPC Tissues (n = 41)	<i>P</i>
Gender			.788
Male	33	29	
Female	12	12	
Age (years)			.949
Median	48	47	
≥50	13	11	
<50	32	30	
Histological type			.875
WHO type II	6	5	
WHO type III	39	36	
Primary tumor (T) stage			.942
T1	10	8	
T2	23	22	
T3	10	10	
T4	2	1	
Lymph node metastasis			.662
Negative	31	30	
Positive	14	11	
Clinical stage			.987
II	12	11	
III	27	25	
IV	6	5	

Abbreviations: NPC, nasopharyngeal carcinoma; WHO, World Health Organization.

Immunostaining was blindly evaluated by 2 investigators in an effort to provide a consensus on staining patterns under light microscopy. A quantitative score was calculated by adding the score of staining intensity and the score of staining area for each case to assess the expression levels of the proteins as previously described by us.¹⁰ At least 10 high-power fields were randomly chosen and >1000 cells were counted for each section. Firstly, a quantitative score was calculated by estimating the percentage of immunopositive cells: 0, no staining of cells in any microscopic fields; 1+, <30% of tissue stained positive; 2+, between 30% and 60% stained positive; and 3+, >60% stained positive. Secondly, the intensity of staining was scored through evaluating the average staining intensity of the positive cells (0, no staining; 1+, mild staining; 2+, moderate staining; 3+, intense staining). Finally, a total score (ranging from 0 to 6) was obtained via adding the area score and the intensity score for each case. A combined staining score of ≤2 was considered to be low staining (negative expression); a score between 3 and 4 was considered to be moderate staining (expression) and that between 5 and 6 was considered to be strong staining (high expression).

Western Blotting

Two NPC cell lines (CNE2-IR and CNE2) were used for Western blotting as previously described.¹¹ Briefly, 30 μg of lysates were separated by 8% sodium dodecyl sulfate

polyacrylamide gel electrophoresis and transferred to polyvinylidene difluoride membrane (Millipore, Bedford, Massachusetts). Blots were incubated with primary anti-ANXA1 antibody (1:500; Sigma-Aldrich) overnight at 4°C, followed by incubation with a horseradish peroxidase-conjugated secondary antibody (1:3000; Amersham Biosciences, Piscataway, New Jersey) for 1 hour at room temperature. The signal was visualized with an enhanced chemiluminescence detection reagent (Thermo Scientific, Rockford, Illinois) and quantitated by densitometry using ImageQuant image analysis system (Storm Optical Scanner; Molecular Dynamics Inc, Sunnyvale, California). β-actin was simultaneously detected with mouse anti-β-actin antibody (1:3000; Sigma) as a loading control.

Stable Transfection With ANXA1 Short Hairpin RNA Plasmid Into CNE2 Cells

Annexin A1 short hairpin RNA (shRNA) plasmid pLKO.1-ANXA1-shRNAs and backbone vector pLKO.1 were purchased from GE Healthcare Life Sciences (Shanghai, China). For stable transfection, 1×10^7 CNE2 cells were transfected with pLKO.1-ANXA1-shRNA or pLKO.1 with Lipofectamine 2000 reagent (Invitrogen), respectively, according to the manufacturer's instructions. After 14 days of selection in DMEM medium containing 1.0 μg/mL puromycin (Invitrogen), individual puromycin-resistant cell was isolated and cultured for proliferation. The expression of ANXA1 in these clones was determined by Western blotting. The CNE2 cells were named CNE2-shANXA1 or CNE2-pLKO.1 after transfected with pLKO.1-ANXA1-shRNAs or pLKO.1-control-shRNA, respectively.

Construction of CNE2-shANXA1 Xenograft Mouse Model

Animal experiments were approved by the institutional review boards of the Central South University and conducted in accordance with the National Institutes of Health Guide for the Care and Use of Laboratory Animals. CNE2-shANXA1, CNE2-pLKO.1, and CNE2 cells (1×10^7) resuspended in 150 μL normal saline were injected subcutaneously into the flank of 6-week-old nude mice, respectively. Tumor growth was monitored via daily measurements of tumor diameters with a Vernier caliper. When the tumor volumes reached approximately 50 mm³, with a modified linear accelerator, a total dose of 10 Gy ionizing radiation (IR) was delivered to the tumor at 2 Gy per fraction per day in 5 consecutive days. After radiation, the general characteristics of the xenograft model mice were observed. The maximum diameter (length) and minimum diameter (width) of the tumor were measured with a Vernier caliper, and the tumor volume was calculated according to the formula (tumor volume = length × width²/2). Two weeks postirradiation, the mice were killed by CO₂ asphyxiation, and their tumors were excised, weighted, fixed, and embedded in paraffin for terminal deoxynucleotidyl transferase-mediated dUTP nick end labeling (TUNEL) and immunohistochemical staining.

Terminal Deoxynucleotidyl Transferase-Mediated dUTP Nick End Labeling Assay

A TUNEL assay was performed to detect apoptotic cells with formalin-fixed and paraffin-embedded tissue sections of xenograft tumors after irradiation with *in situ* cell death detection kit (Roche, Basel, Switzerland), according to the manufacturer's instruction. A positive reaction was defined as the intracellular distribution of brown coarse particles or the diffuse distribution of brownish yellow fine particles. The stained cells were counted under the light microscope. Quantitative evaluation of apoptotic cells was done via examining the sections in 10 random microscopic fields and counting the number of TUNEL-positive cancer cells among 1000 carcinoma cells under the light microscope.

Immunohistochemistry Assay for Phospho-DNA-Dependent Protein Kinase and γ -H2AX

Immunohistochemical staining of phospho-DNA-dependent protein kinase (DNA-PKcs' S2056) and γ H2AX (phospho-S139) was performed on 4- μ m formalin-fixed and paraffin-embedded tissue sections with anti-phospho-DNA PKcs (1:200; Abcam, USA) or anti- γ H2AX antibody (1:500; Abcam, USA), respectively. Immunohistochemistry and evaluation of staining were performed as previously described.¹¹

Reactive Oxygen Species Assay

Generation of intracellular ROS was measured with the fluorescent probe 2',7'-dichlorofluorescein diacetate (DCF-DA; Invitrogen). After treated with irradiation (2 Gy), cells were incubated with the fluorescent probe DCF-DA for 30 minutes. The intensity of DCF-DA fluorescence was determined by using a FACScan flow cytometer (Becton Dickinson, Franklin Lakes, New Jersey), with an excitation wavelength of 480 nm and an emission wavelength of 530 nm.

Comet Assay

DNA damage was estimated with comet assay (namely alkaline single-cell gel electrophoresis assay) according to the report described by Mallebrera *et al.*¹² Briefly, CNE2-shANXA1, CNE2-pLKO.1, and CNE2 cells were seeded into 6-well plates. After the cells were cultured overnight, they were treated with irradiation (2 Gy). Then, the cells were embedded in 0.8% low melting point agarose, transferred to slides, and lysed. The slides were then immersed in an alkaline solution (300 mM NaOH, 1 mM Na₂EDTA, pH 13) for 40 minutes at room temperature. The electrophoresis was run in the same solution at 0.7 V/cm (voltage across the platform) and 300 mA for 24 minutes. After electrophoresis, the slides were washed twice in neutralization buffer, dried in 96% ethanol, and stained with 20 mg/mL propidium iodide). The analysis was performed with a fluorescence microscope (Nikon Eclipse E800, Melville, NY) at $\times 400$ magnification.

Statistical Analysis

The data were obtained from 3 independent experiments. Statistically significant differences between the 2 groups were assessed with the Student *t* test using Statistical Package for Social Sciences 18.0 (SPSS Inc, Chicago, Illinois). The data were expressed as the standard deviation. Value of $P < .05$ was considered to indicate a statistically significant difference.

Results

Expression of ANXA1 in the NPC Tissue and Cell Line With Radioresistance

Immunohistochemistry was done on formalin-fixed and paraffin-embedded tissue specimens including 41 radioresistant NPC tissues and 45 radiosensitive NPC tissues. There were no significant differences in clinical characteristics between patients with radioresistant and radiosensitive NPC (Table 1, $P < .05$). Immunohistochemical analysis demonstrated that ANXA1 protein distribution was primarily observed in the cytoplasm and nucleus, and ANXA1 protein expression decreased significantly in the radioresistant NPC tissues compared with its abundance in the radiosensitive NPC tissues (Figure 1A). Among the 41 radioresistant NPC tissue samples, 48.8% (20/41) of samples were negative stain (low expression) and 51.2% (21/41) of samples were positive stain (diffuse cytoplasmic staining, moderate and high expression). However, there were 13.3% (6/45) negative stain (low expression) and 86.7% (39/45) positive stain (strong diffuse cytoplasmic staining and nuclear staining) among the 45 radiosensitive NPC tissue samples (Table 2, $P < .05$). Western blotting was done to detect the expression level of ANXA1 in NPC cell lines CNE2-IR and CNE2, respectively. As shown in Figure 1B, there was a significantly lower expression of ANXA1 in CNE-2-IR than that in CNE2 (control cells; $P < .05$). The results indicated that the reduction in protein of ANXA1 is related to radioresistance in NPC.

Establishment of CNE2-shANXA1 Cell Line With Knockdown of ANXA1

To know whether downregulation of ANXA1 is involved in NPC radioresistance, the CNE2 cells were respectively transfected with ANXA1 shRNA plasmid pLKO.1-ANXA1-shRNAs or backbone vector pLKO.1 with puromycin screening; some clones of those cell lines grew after 14 days. After expanded culture, Western blotting was used to detect the expression level of ANXA1 in the NPC cell lines. As shown in Figure 1C, the expression level of ANXA1 in CNE2-shANXA1 was significantly lower than that in CNE2-pLKO.1 ($P < .01$). There were no obvious differences in ANXA1 expression levels between CNE2 and CNE2-pLKO.1, however ($P > .05$). Therefore, we generated stably transfected human NPC cell line CNE2-shANXA1 with knockdown of ANXA1 gene. The stable NPC cell lines could be used in the following experiments.

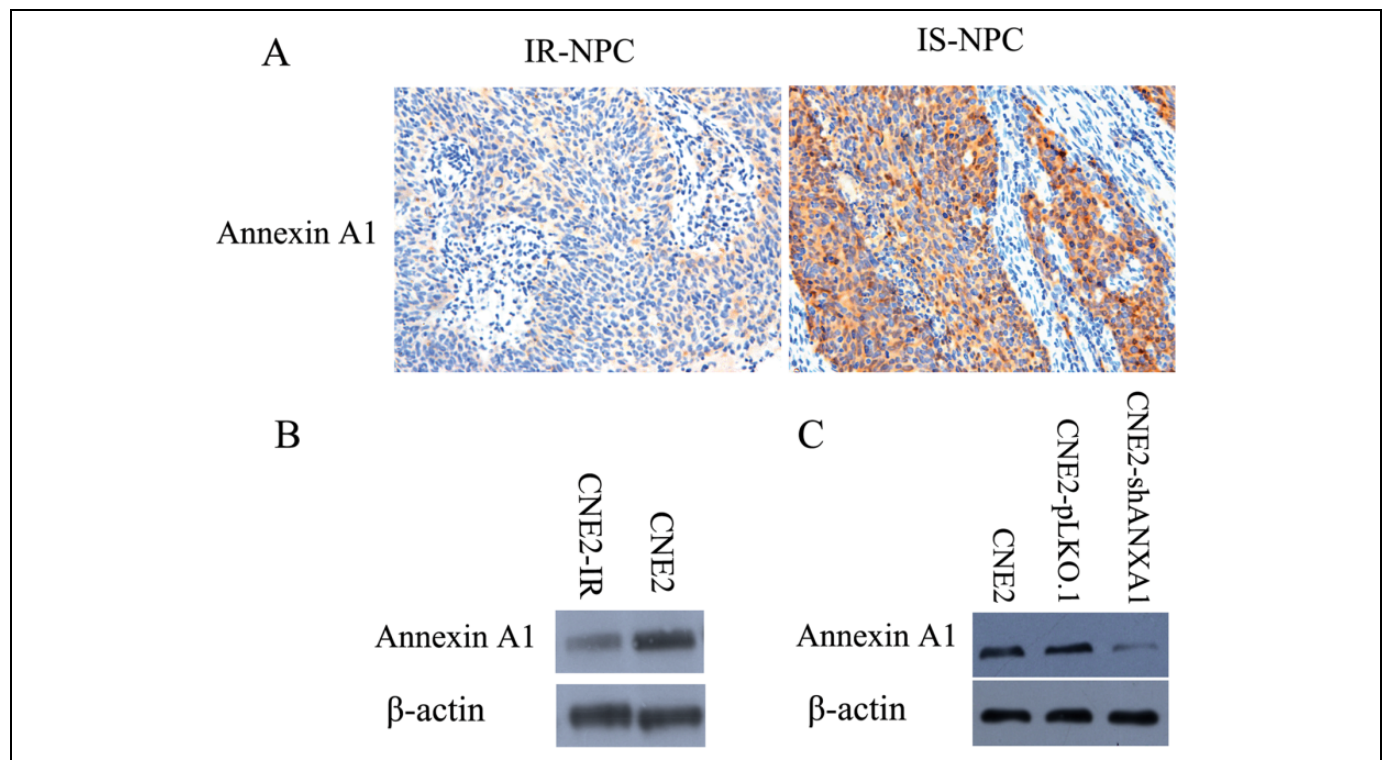


Figure 1. The expression of annexin A1 in NPC tissues and NPC cell lines. A, Immunohistochemistry assay was performed to detect the expression of annexin A1 protein in NPC tissues. B, Western blotting was done to detect the expression level of annexin A1 in the 2 NPC cell lines CNE2-IR and CNE2. C, Western blotting was done to detect the expression level of annexin A1 in CNE2, CNE2-pLKO.1, and CNE2 shANXA1. IR-NPC indicates irradiation resistant NPC tissues; IS-NPC, irradiation sensitive NPC tissues; NPC, nasopharyngeal carcinoma.

Table 2. Expression of Annexin A1 in the Radioresistant and Radiosensitive NPC Tissues.

NPC Tissues	n	Score			P
		Low (0-2)	Moderate (3-4)	High (5-6)	
Radioresistance	41	20	9	12	.0001 ^a
Radiosensitivity	45	6	14	25	

Abbreviation: NPC, nasopharyngeal carcinoma.

^a $P < .05$ with χ^2 test, radioresistant versus radiosensitive NPC tissues.

Knockdown of ANXA1 Increases Radioresistance in CNE2 Xenograft Model

We generated a xenograft model to determine the effects of ANXA1 on NPC radioresistance *in vivo*. CNE2-shANXA1, CNE2-pLKO.1, and CNE2 cells were injected subcutaneously into the flank of nude mice, respectively. In the 14th day post-injection, tumors formation, *in vivo* irradiation directed to the tumors was performed (2 Gy daily dose for 5 days). The tumors in CNE2-shANXA1 mice presented a faster growth than that in CNE2-pLKO.1 and CNE2 mice (Figure 2A and B). All mice of xenograft model were killed for 2 weeks postirradiation to examine the final tumor volume and weight. The results showed that the tumor volume and weight were significantly larger or heavier in CNE2-shANXA1 mice compared with that in CNE2-pLKO.1 and CNE2 mice postirradiation (Figure 2).

However, there was no significant difference in tumor growth, tumor volume, and weight between CNE2-pLKO.1 and CNE2 mice (Figure 2).

To investigate how ANXA1 contributes to radioresistance in NPC *in vivo*, we performed the TUNEL assays on xenograft tumor sections. The results revealed knockdown of ANXA1 significantly inhibited radiation-induced apoptosis (Figure 3). Moreover, we detected the key molecular markers involved in DNA damage and repair. The results showed that the phosphorylation level of H2AX significantly decreased (Figure 4C, left; Figure 4D, upper); however, the accumulation of DNA-PKs markedly increased in CNE2-shANXA1 tumor compared with that in CNE2-pLKO.1 and CNE2 tumor postirradiation (Figure 4C, right; Figure 4D, bottom). In brief, our data showed that ANXA1 significantly enhanced radioresistance in NPC cell *in vivo*.

Knockdown of ANXA1 Reduced DNA Damage in CNE2-shANXA1 Cell Line

The ROS levels in CNE2-shANXA1, CNE2-pLKO.1, and CNE2 cells after 2 Gy irradiation were detected with the fluorescent probe DCF-DA. As shown in Figures 4A, CNE2-shANXA1 cells contained significantly lower concentrations of ROS than CNE2-pLKO.1 and CNE2 cells, whereas the level of ROS in CNE2-pLKO.1 and CNE2 cells had not differed

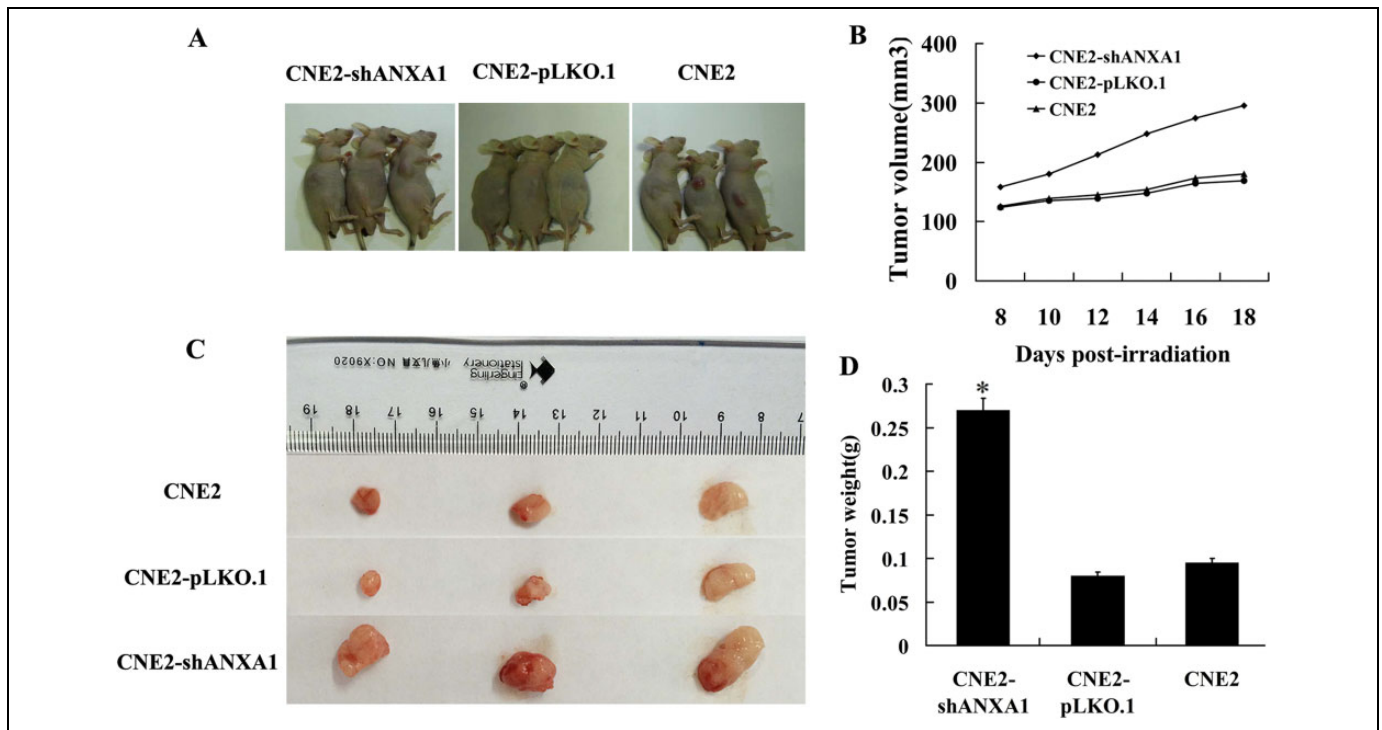


Figure 2. The effects of knockdown of annexin A1 on tumor growth in CNE2 xenograft model after irradiation. A, The images of nude mice in xenograft model and the tumors generated by CNE2-shANXA1, CNE2-pLKO.1, and CNE2 cells after 10 Gy irradiation. B, The growth curves of the tumors after irradiation. C, Two weeks after irradiation, the mice were killed, and the tumors were photographed. D, The average weights of the tumors after irradiation at the time of killing. Data are represented as the mean (standard deviation). * $P < .05$.

significantly after IR. Annexin A1 knockdown markedly decreased intracellular ROS levels and inhibited radiation-induced DNA damage.

To further confirm the role of ANXA1 in radioresistance in NPC cells, we performed the comet assays to assess the extent of DNA damage in both the CNE2-shANXA1 cells and the control cells when they were exposed to radiation. Compared with the cells before irradiation, it showed nearly no DNA damage (Figure 4B, left), and the cells that were exposed to 2 Gy of irradiation exhibited “comet tails.” However, the average tail length in CNE2-shANXA1 cells was significantly shorter than that in CNE2-pLKO.1 and CNE2 cells (Figure 4B, right). These results illustrated that knockdown of ANXA1 could significantly reduce the levels of DSBs (Figure 4B). Hence, it implied that ANXA1 might play a crucial role in radioresistance in NPC.

Discussion

Annexin A1 exhibits tumor type-specific patterns of expression and localization. It plays multiple important roles in tumor development, proliferation, invasion, and metastasis.³⁻⁵ The expression of ANXA1 is observed during the development and progression in many cancers. The reduction in the expression of ANXA1 is significantly associated with poor differentiation and pathologic differentiation grade in oral squamous cell carcinoma. Overexpression of ANXA1 significantly reduced

cellular proliferation, whereas its downregulation increased proliferation in oral squamous cell carcinoma lines and nude mice.⁷ The expression of ANXA1 was associated with higher grades of differentiation or less aggressive tumors in HNSCC, suggesting that ANXA1 might act as a tumor suppressor.⁶ The role of ANXA1 in radioresistance has been found in HNSCC. As a direct target of miR-196a in head and neck cancer cell lines, knockdown of ANXA1 led to enhance cellular proliferation, survival, and migration. Knockdown of ANXA1 in HNSCC exhibited similar phenotypic effects in miR-196a overexpression. Annexin A1 silencing resulted in some resistance to irradiation.¹³ Collectively, these findings suggested the oncogenic effect of miR-196a is partly regulated through the suppression of ANXA1. In our previous study, we had found that ANXA1 downregulation significantly enhanced clonogenic survival and cell growth after CNE2 cells treated with IR increased number of cells in the S phase and decreased IR-induced apoptosis.¹⁴ Here, our results elucidated that the expression of ANXA1 protein significantly decreased in the radioresistant NPC tissues and cell line compared to its abundance in the radiosensitive NPC tissues and cell line via immunohistochemical analysis and Western blotting. Together, our study indicates that ANXA1 is related to radioresistance in NPC.

Next, we established the CNE2-shANXA1, CNE2-pLKO.1, and CNE2 cells xenograft model to investigate the effect of downregulation of ANXA1 on NPC radioresistance *in vivo*.

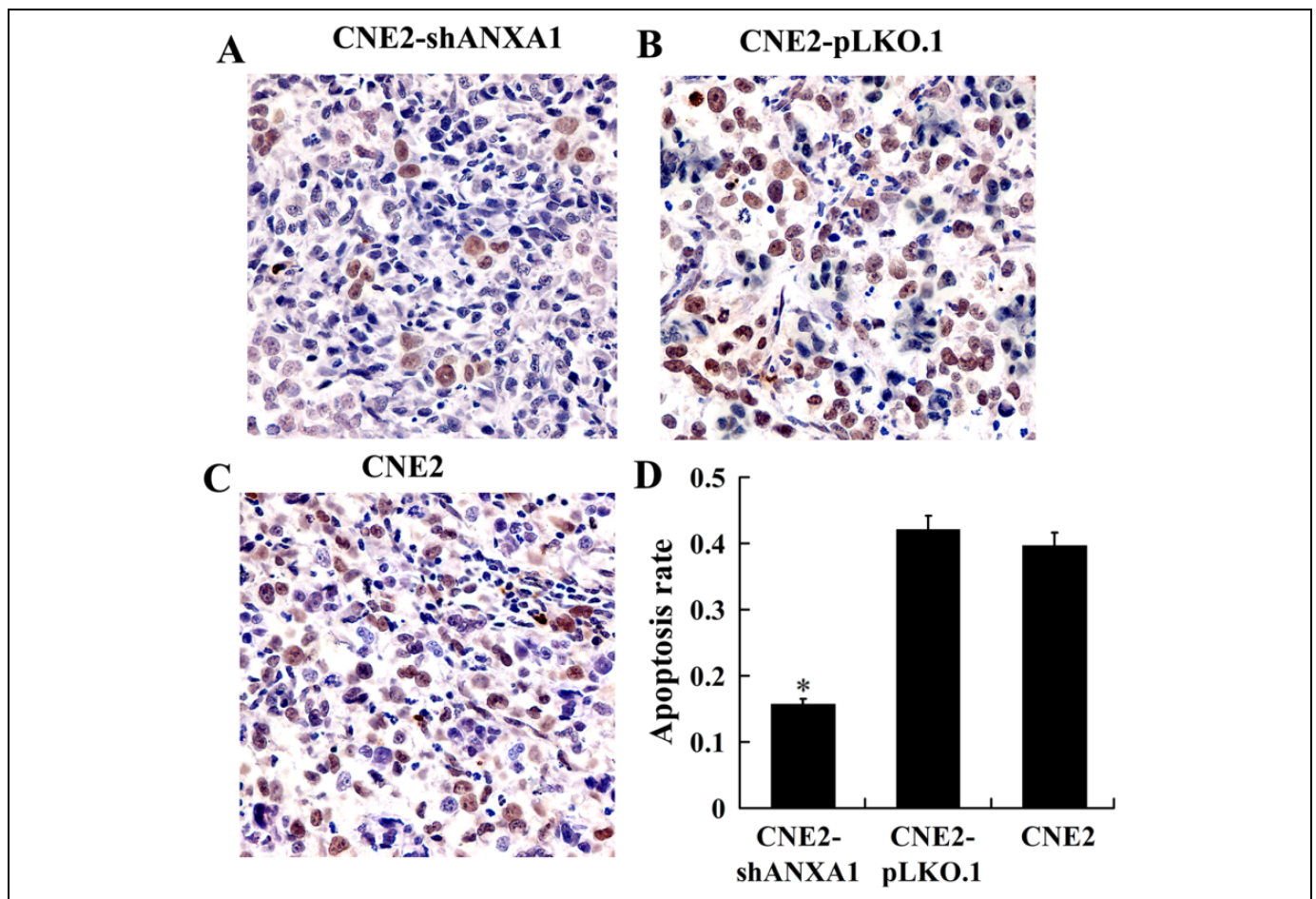


Figure 3. The effects of knockdown of annexin A1 on apoptosis in xenograft tumors. A-C, Representative image of TUNEL detection of apoptotic cells in the tumors generated by CNE2-shANXA1, CNE2-pLKO.1, and CNE2 cells after irradiation. D, A histogram shows percentages of apoptotic cells in the tumors. Data are represented as the mean (standard deviation). * $P < .05$. TUNEL indicates terminal deoxynucleotidyl transferase-mediated dUTP nick end labeling.

The subcutaneous tumors in CNE2-shANXA1 were dramatically larger and heavier than that in CNE2-pLKO.1 and CNE2 postirradiation *in vivo*. It suggested that downregulation of ANXA1 obviously increased the growth rate of xenograft tumors in nude mice postradiotherapy, and the radioresistance of tumors occurred with downregulation of ANXA1 in CNE2-shANXA1 cells was significantly more than that in CNE2-pLKO.1 and CNE2 cells.

Apoptosis is one of crucial role in the cellular death pathway following exposure to irradiation. Previous studies suggest that ANXA1 plays important roles in the DNA damage response¹⁵ linked to proapoptotic effects and regulates apoptosis.⁵ It has been reported that upregulation of endogenous ANXA1 promotes cell death.¹⁶ Restoring ANXA1 expression reduced cell viability and colony formation besides inducing apoptosis in the prostate cancer cell lines.¹⁷ In this study, we found that knockdown of ANXA1 reduced radiation-induced apoptosis in CNE2 cells by using TUNEL assay. It predicts that the downregulation of ANXA1 enhances NPC radioresistance through decreasing apoptosis. Moreover, ANXA1 is believed to inhibit the transcriptional activity of nuclear

factor- κ B via binding directly to p65 subunit.¹⁸ NF- κ B inhibitors were reported to enhance the efficacy of radiotherapy through sensitizing the cancer cells to irradiation by increasing the apoptosis.¹⁹ Hence, knockdown of ANXA1 might significantly inhibit radiation-induced apoptosis in NPC cells. The role of ANXA1 in NPC radiotherapy was possibly dependent on the binding to NF- κ B, but the further investigations over accurate molecular mechanism are required in future studies. Additionally, tumor suppressor p53 protein was recognized as an important checkpoint protein, and it functions mainly as influencing multiple response pathways through transcriptional control of target genes and leading to the diversity of responses to irradiation. p53 protein activates the expression of ANXA1 owing to its binding site in upstream of the proximal CCAAT box. Hence, p53 protein might be related to NPC radioresistance.²⁰ Knockdown of p53 not only decreases NPC radiosensitivity but also reduces expression of ANXA1. Collectively, ANXA1 is likely involved in p53-mediated radioresponse in NPC^{21,22}; the exact molecular biology mechanism is unclear, which needs to be studied further.

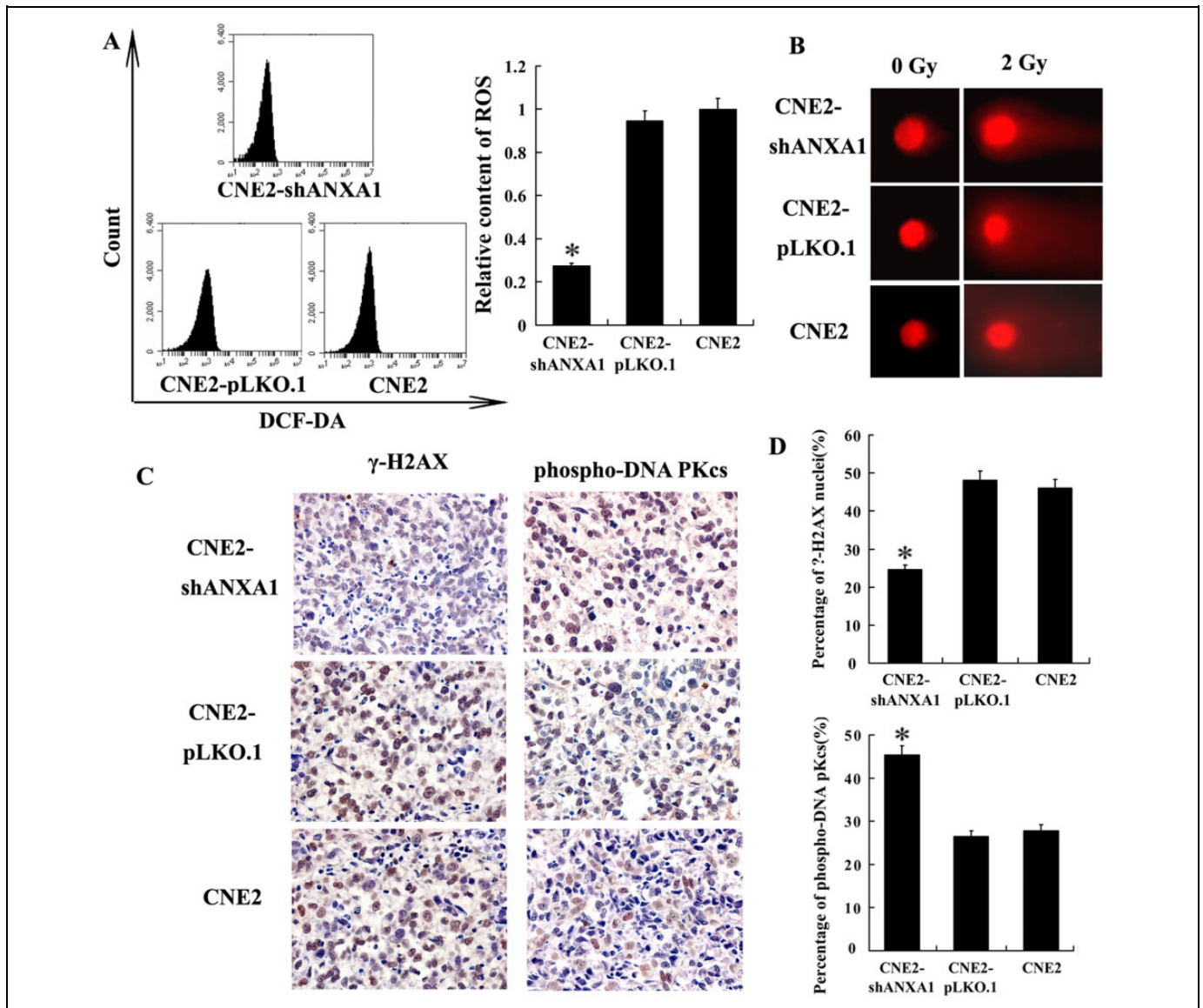


Figure 4. The effects of knockdown of annexin A1 on DNA damage and repair in NPC cells. A, (Left) Flow cytometry detection of ROS levels after irradiation by DCF-DA. A, (Right) A histogram shows the relative content of ROS in CNE2-shANXA1, CNE2-pLKO.1, and CNE2 cells after irradiation. B, The comet assay was performed to detect DNA strand-double breaks in CNE2-shANXA1, CNE2-pLKO.1, and CNE2 cells. Original magnification, $\times 400$. C, (Left) A representative image of immunohistochemical staining of γ H2AX in the tumors generated by CNE2-shANXA1, CNE2-pLKO.1, and CNE2 cells after irradiation. C, (Right) A representative image of immunohistochemical staining of phospho-DNA PKcs in the tumors generated by CNE2-shANXA1, CNE2-pLKO.1, and CNE2 cells after irradiation. D, (Upper) A histogram shows percentages of γ -H2AX positive cells in the tumors. D, (bottom) A histogram shows percentages of phospho-DNA PKcs positive cells in the tumors. Means, standard deviations, and statistical significance are denoted; $*P < .05$. NPC indicates nasopharyngeal carcinoma; ROS, reactive oxygen species.

We measured intracellular ROS levels in CNE2-shANXA1, CNE2-pLKO.1, and CNE2 cells after 2 Gy irradiation with the fluorescent probe DCF-DA because ROS plays an important role in cell apoptosis,²³ which directly triggers DNA damage in cells.²⁴ We found that the level of ROS in CNE2-shANXA1 cells was significantly lower than that in CNE2-pLKO.1 and CNE2 cells after IR. Hence, ANXA1 knockdown might markedly inhibit intracellular ROS levels and reduce DNA damage postirradiation.

Ionizing radiation leads primarily to DNA damage (DSBs) and triggers the activation of DNA damage and repair pathways.²⁵ Double-strand breaks are correlated with tumor radiosensitivity and are the primary cause of postradiotherapy cell death.^{26,27} The comet assay (single-cell gel electrophoresis) was reported to be the most rapid and sensitive method for detecting DNA damage in individual cells.^{28,29} Under alkaline conditions, damaged DNA was travelling during electrophoresis from the nucleus toward the anode, generating a shape of a

“comet” with a head (cell nucleus with intact DNA) and a tail (released or broken DNA). This assay is capable of detecting DSBs in the tail. In samples of human bladder cancer tissue irradiated *ex vivo*, radiation-induced DNA damage levels were measured with this assay, and the extent of comet formation was found to correlate with cell killing.³⁰ Therefore, we assessed the DNA damage in NPC cells with comet assay under alkaline pH. We observed that total DNA damage was significantly higher in CNE2-pLKO.1 and CNE2 cells than that in CNE2-shANXA1 cells postirradiation.

Phosphorylation of histone H2AX, which is a sensitive reporter for DNA DSBs,^{26,31} is positively associated with the accumulation of γ -H2AX foci and DSBs.³² Detection of the formation of γ -H2AX foci has emerged as a highly sensitive and specific molecular marker for DNA damage in the context of irradiation. To detect DNA damage in NPC cells after irradiation, the foci that form at DNA DSBs were detected with antibody against γ -H2AX in xenograft tumors cells via immunohistochemistry. The data revealed that knockdown of ANXA1 could decrease the quantification of γ -H2AX foci in the CNE2-shANXA1 compared with that in the CNE2-pLKO.1 and CNE2. The results of the formation of γ -H2AX foci were in line with that with the comet assay, which supported that knockdown of ANXA1 inhibits DNA fragmentation in NPC cells postirradiation. These results demonstrated that knockdown of ANXA1 could reduce significantly the levels of DSBs and indicated that ANXA1 might play a crucial role in radioresistance in NPC.

DNA-dependent protein kinase is confirmed to play an important role in the nonhomologous end-joining pathway in DNA DSB repair.^{33,34} DNA-dependent protein kinase recruited by DSBs took part in DNA repair when DSBs were induced by irradiation. The activation of DNA-PKcs was critical for DNA DSBs repair. In this study, to further elucidate the underlying mechanism involved in knockdown of ANXA1 on cellular DNA repair, we detected the expression of the phospho-DNA-PKcs with antibody against phospho-DNA-PKcs in xenograft tumors cells postirradiation via immunohistochemistry. The results showed that knockdown of ANXA1 could increase radiation-induced accumulation of DNA-PKcs with immunostaining. More phospho-DNA-PKcs were positively related to DSBs repair. Thus, increasing DNA DSBs repair is suggested to increase the radioresistance in NPC. These results suggest that knockdown of ANXA1 inhibits DNA damage through decreasing the generation of intracellular ROS and the formation of γ -H2AX, promotes DNA repair through increasing DNA-PKcs activity, and therefore accentuates the radioresistance in NPC cells.

In conclusion, ANXA1 is critical for radioresponse in NPC cells. Knockdown of ANXA1 markedly increased the radioresistance in NPC cells through inhibiting the generation of intracellular ROS, reducing DNA damage, decreasing the quantification of γ -H2AX, increasing DNA-PKcs activity, and inducing less apoptosis. The knockdown of ANXA1 increased the radioresistance in NPC cells, which was linked to decreasing radiation-induced DNA damage, enhancing DNA repair,

and inhibiting apoptosis. Our findings suggest that ANXA1 could be a radiosensitizing target in NPC and provide novel insights on investigating further molecular mechanisms underlying the role of ANXA1 in NPC radiosensitization.

Declaration of Conflicting Interests

The author(s) declared no potential conflicts of interest with respect to the research, authorship, and/or publication of this article.

Funding

The author(s) disclosed receipt of the following financial support for the research, authorship, and/or publication of this article: This research program was supported by National Natural Science Foundation of China (81272959, 81470130) and a grant from the Educational Committee of Hunan Province (17A188).

References

1. Ho JH. An epidemiologic and clinical study of nasopharyngeal carcinoma. *Int J Radiat Oncol Biol Phys.* 1978;4(3-4):182-198.
2. Liao LQ, Yan HH, Mai JH, et al. Radiation-induced osteosarcoma of the maxilla and mandible after radiotherapy for nasopharyngeal carcinoma. *Chin J Cancer.* 2016;35(1):89.
3. Lim LH, Pervaiz S. Annexin 1: the new face of an old molecule. *FASEB J.* 2007;21(4):968-975.
4. Guo C, Liu S, Sun MZ. Potential role of Anxa1 in cancer. *Future Oncol.* 2013;9(11):1773-1793.
5. Biao Xue R, Xiguang C, Shuanying Y. Annexin A1 in malignant tumors: current opinions and controversies. *Int J Biol Markers.* 2014;29(1):e8-e20.
6. Garcia Pedrero JM, Fernandez MP, Morgan RO, et al. Annexin A1 down-regulation in head and neck cancer is associated with epithelial differentiation status. *Am J Pathol.* 2004;164(1):73-79.
7. Rodrigo JP, Garcia-Pedrero JM, Fernandez MP, Morgan RO, Suárez C, Herrero A. Annexin A1 expression in nasopharyngeal carcinoma correlates with squamous differentiation. *Am J Rhinol.* 2005;19(5):483-487.
8. Huang DH, Tian YQ, Qiu YZ, Fan SQ, Li GY. A study on PCNA and survivin as the molecule marks to predict tumor radiosensitivity of nasopharyngeal carcinoma. *J Tong Univ (Med Sci).* 2006; 27(5):39-42.
9. Feng XP, Yi H, Li MY, et al. Identification of biomarkers for predicting nasopharyngeal carcinoma response to radiotherapy by proteomics. *Cancer Res.* 2010;70(9):3450-3462.
10. Zeng GQ, Zhang PF, Deng X, et al. Identification of candidate biomarkers for early detection of human lung squamous cell cancer by quantitative proteomics. *Mol Cell Proteomics.* 2012;11(6): M111.013946.
11. Tan X, Liao L, Wan YP, et al. Downregulation of selenium-binding protein 1 is associated with poor prognosis in lung squamous cell carcinoma. *World J Surg Oncol.* 2016;14:70.
12. Mallebrera B, Juan-Garcia A, Font G, Ruiz MJ. Mechanisms of beauvericin toxicity and antioxidant cellular defense. *Toxicol Lett.* 2016;246:28-34.
13. Suh YE, Raulf N, Gäken J, et al. MicroRNA-196a promotes an oncogenic effect in head and neck cancer cells by suppressing

- annexin A1 and enhancing radioresistance. *Int J Cancer*. 2015; 137(5):1021-1034.
14. Huang L, Liao L, Wan Y, et al. Downregulation of Annexin A1 is correlated with radioresistance in nasopharyngeal carcinoma. *Oncol Lett*. 2016;12(6):5229-5234.
15. Swa HL, Blackstock WP, Lim LH, Gunaratne J. Quantitative proteomics profiling of murine mammary gland cells unravels impact of annexin 1 on DNA damage response, cell adhesion and migration. *Mol Cell Proteomics*. 2012;11(8):381-393.
16. Tabe Y, Jin L, Contractor R, et al. Novel role of HDAC inhibitors in AML1/ETO AML cells: activation of apoptosis and phagocytosis through induction of annexin A1. *Cell Death Differ*. 2007; 14(8):1443-1456.
17. Hsiang CH, Tunoda T, Whang YE, Tyson DR, Ornstein DK. The impact of altered annexin I protein levels on apoptosis and signal transduction pathways in prostate cancer cells. *Prostate*. 2006; 66(13):1413-1424.
18. Zhang Z, Huang L, Zhao W, Rigas B. Annexin 1 induced by anti-inflammatory drugs binds to NF-kappaB and inhibits its activation: anticancer effects in vitro and in vivo. *Cancer Res*. 2010; 70(6):2379-2388.
19. Kuo YC, Lin WC, Chiang IT, et al. Sorafenib sensitizes human colorectal carcinoma to radiation via suppression of NF-kappaB expression in vitro and in vivo. *Biomed Pharmacother*. 2012; 66(1):12-20.
20. Gudkov AV, Komarova EA. The role of p53 in determining sensitivity to radiotherapy. *Nat Rev Cancer*. 2003;3(2):117-129.
21. Fei P, El-Deiry WS. P53 and radiation responses. *Oncogene*. 2003;22(37):5774-5783.
22. Lecona E, Barrasa JI, Olmo N, Llorente B, Turnay J, Lizarbe MA. Upregulation of annexin A1 expression by butyrate in human colon adenocarcinoma cells: role of p53, NF-Y, and p38 mitogen-activated protein kinase. *Mol Cell Biol*. 2008;28(15):4665-4674.
23. He L, Chen T, You Y, et al. A cancer-targeted nanosystem for delivery of gold(III) complexes: enhanced selectivity and apoptosis-inducing efficacy of a gold(III) porphyrin complex. *Angew Chem Int Ed Engl*. 2014;53(46):12532-12536.
24. He L, Lai H, Chen T. Dual-function nanosystem for synergetic cancer chemo-/radiotherapy through ROS-mediated signaling pathways. *Biomaterials*. 2015;51:30-42.
25. Ashwell S, Zabludoff S. DNA damage detection and repair pathways—recent advances with inhibitors of checkpoint kinases in cancer therapy. *Clin Cancer Res*. 2008;14(13): 4032-4037.
26. Zheng H, Chen ZW, Wang L, et al. Radioprotection of 4-hydroxy-3,5-dimethoxybenzaldehyde (VND3207) in culture cells is associated with minimizing DNA damage and activating Akt. *Eur J Pharm Sci*. 2008;33(1):52-59.
27. Mah LJ, Vasireddy RS, Tang MM, Georgiadis GT, El-Osta A, Karagiannis TC. Quantification of gammaH2AX foci in response to ionising radiation. *J Vis Exp*. 2010;38(38):174-192.
28. Collins AR. The comet assay for DNA damage and repair: principles, applications, and limitations. *Mol Biotechnol*. 2004;26(3): 249-261.
29. McKenna DJ, McKeown SR, McKelvey-Martin VJ. Potential use of the comet assay in the clinical management of cancer. *Mutagenesis*. 2008;23(3):183-190.
30. Bowman KJ, Al-Moneef MM, Sherwood BT, et al. Comet assay measures of DNA damage are predictive of bladder cancer cell treatment sensitivity in vitro and outcome in vivo. *Int J Cancer*. 2014;134(5):1102-1111.
31. Rogakou EP, Pilch DR, Orr AH, Ivanova VS, Bonner WM. DNA double-stranded breaks induce histone H2AX phosphorylation on serine 139. *J Biol Chem*. 1998;273(10):5858-5868.
32. Sone K, Piao L, Nakakido M, et al. Critical role of lysine 134 methylation on histone H2AX for γ -H2AX production and DNA repair. *Nat Commun*. 2014;5:5691.
33. Chan DW, Chen BP, Prithivirajasingh S, et al. Autophosphorylation of the DNA-dependent protein kinase catalytic subunit is required for rejoining of DNA double-strand breaks. *Genes Dev*. 2002;16(18):2333-2338.
34. Xing M, Yang M, Huo W, et al. Interactome analysis identifies a new paralogue of XRCC4 in non-homologous end joining DNA repair pathway. *Nat Commun*. 2015;6:6233.